

Possible pressure-induced insulator-to-metal transition in low-dimensional TiOClC. A. Kuntscher,^{1,*†} S. Frank,^{1,*} A. Pashkin,^{1,*} M. Hoinkis,^{2,3} M. Klemm,² M. Sing,³ S. Horn,² and R. Claessen³¹*Physikalisches Institut, Universität Stuttgart, Pfaffenwaldring 57, D-70550 Stuttgart, Germany*²*Experimentalphysik 2, Universität Augsburg, D-86135 Augsburg, Germany*³*Experimentelle Physik 4, Universität Würzburg, D-97074 Würzburg, Germany*

(Received 2 January 2006; revised manuscript received 1 August 2006; published 3 November 2006)

We studied the transmittance and reflectance of the low-dimensional Mott-Hubbard insulator TiOCl in the infrared and visible frequency range as a function of pressure. The strong suppression of the transmittance and the abrupt increase of the near-infrared reflectance in the high-pressure range suggest a pressure-induced insulator-to-metal transition. The pressure-dependent frequency shifts of the orbital excitations, as well as the pressure dependences of the charge gap and the spectral weight of the optical conductivity above the phase transition, are presented.

DOI: [10.1103/PhysRevB.74.184402](https://doi.org/10.1103/PhysRevB.74.184402)

PACS number(s): 71.30.+h, 78.30.-j, 62.50.+p

I. INTRODUCTION

Low-dimensional titanium-oxychloride (TiOCl) evoked interest already 13 years ago as a two-dimensional magnetically frustrated system, which upon doping might form a resonating valence bond state and even show unconventional superconductivity.¹ Recently, TiOCl again has encountered vital interest as a spin-Peierls system with puzzling properties: Magnetic susceptibility measurements showed a Bonner-Fisher-type behavior at high temperature typical for a one-dimensional spin-1/2 Heisenberg chain, with a relatively high exchange coupling.^{2,3} At low temperature a non-magnetic phase accompanied by a doubling of the unit cell was observed, suggesting a spin-Peierls state with a dimerization of the chains of Ti atoms along the *b* axis.⁴ This picture is, however, complicated by the occurrence of an additional second-order phase transition at $T_{c2}=91$ K above the first-order spin-Peierls transition at $T_{c1}=67$ K.

In order to explain the deviations from a canonical spin-Peierls picture, the influence of strong orbital fluctuations with a near degeneracy of the lowest-lying 3*d* orbitals was proposed.^{3,5-7} However, recent cluster calculations combined with transmittance measurements^{8,9} could rule out such a scenario: A significant crystal field splitting of the t_{2g} orbitals was found, which indicates the quenching of the orbital degree of freedom. This is in accordance with other recent results obtained by angle-resolved photoemission spectroscopy (ARPES) and electron spin resonance (ESR).^{10,11} Within this picture, the second-order phase transition at T_{c2} is interpreted in terms of a transition to an incommensurate spin-Peierls state with a subsequent lock-in transition to a commensurate dimerized state below T_{c1} .^{8,12,13} The importance of frustration of the interchain interactions in the incommensurate phase was pointed out,⁸ in agreement with the earlier proposal of TiOCl being a two-dimensional frustrated system.¹

This brings us back to the earlier idea of a resonating valence bond state in doped TiOCl. TiOCl is a Mott-Hubbard insulator, where the Ti 3*d* shell is occupied by one electron, and due to electronic correlations, these charge carriers are localized on site. However, the carrier localization effects should be relatively weak because of the high nearest-

neighbor exchange coupling.^{2,3} It was suggested that TiOCl is close to an insulator-to-metal transition and furthermore might exhibit exotic superconductivity upon doping.^{1,2,14} Unfortunately, up to now doping of TiOCl could not be achieved.

In our study, we followed another route to search for a possible metallic state of TiOCl: namely, via the application of high external pressure. Indeed, we find large pressure-induced changes in the optical response: a strong suppression of the transmittance in the infrared and visible range, accompanied by a change of the sample color from red to black, and an abrupt increase of the near-infrared reflectance at high pressure. All these findings suggest the occurrence of an insulator-to-metal transition in TiOCl under pressure.

II. EXPERIMENT

The crystal structure of TiOCl consists of strongly distorted [TiO₄Cl₂] octahedra.¹⁵ A different view of the structure is that of buckled Ti-O bilayers parallel to the *ab* plane and separated by Cl ions. Single crystals of TiOCl were synthesized by chemical vapor transport from TiCl₃ and TiO₂.¹⁵ The crystal quality was validated by x-ray diffraction, specific heat, and magnetic susceptibility measurements.

A diamond anvil cell (DAC) was used for the generation of pressures up to 18 GPa. For the transmission measurements various pressure-transmitting media were used [CsI, methanol:ethanol (4:1)-mixture, argon]. The results qualitatively agree,¹⁶ but the pressure-induced effects occur at lower pressure ($\Delta P \approx 4$ GPa) for CsI powder due to less hydrostatic conditions, as expected.¹⁷ For the reflectance measurements finely ground CsI powder was used as pressure-transmitting medium to ensure direct contact of the sample with the diamond window. For each transmittance and reflectance measurement a small piece (about 80 $\mu\text{m} \times 80 \mu\text{m}$) was cut from single crystals with a thickness of $\leq 5 \mu\text{m}$ and placed in the hole of a steel gasket. The pressure was determined by the ruby luminescence method.¹⁸

Pressure-dependent transmittance and reflectance experiments were conducted at room temperature using a Bruker IFS 66v/S FT-IR spectrometer with an infrared microscope (Bruker IRscope II). The reproducibility of the results was

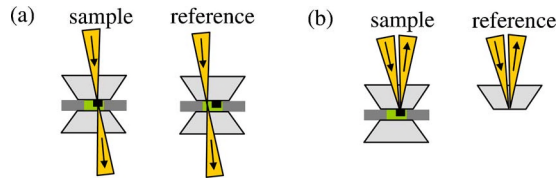


FIG. 1. (Color online) Geometry for high-pressure (a) transmittance and (b) reflectance measurements of the sample in the diamond anvil cell.

ensured by several experimental runs on different pieces of eight crystals. The pressure-dependent transmittance was studied in a wide frequency range (2000–22000 cm^{-1}) for the polarization directions $\mathbf{E}||a, b$. We measured the intensity $I_s(\omega)$ of the radiation transmitting the sample [see Fig. 1(a)]; as reference, for each pressure we focused the incident radiation spot on the empty space in the gasket hole next to the sample and obtained the transmitted intensity $I_r(\omega)$. The ratio $T(\omega) = I_s(\omega)/I_r(\omega)$ is a measure of the transmittance of the sample, and the corresponding absorbance is calculated according to $A = \log_{10}(1/T)$; A is a measure of the optical conductivity.

Pressure-dependent reflectance measurements were carried out in the frequency range ≈ 3000 – $11\,000$ cm^{-1} for $\mathbf{E}||a, b$. Reflectance spectra R_{s-d} of the sample with respect to diamond were obtained by measuring the intensity $I_{s-dia}(\omega)$ reflected at the interface between the sample and diamond anvil [see Fig. 1(b)]. As reference, the intensity $I_{dia}(\omega)$ reflected from the inner diamond-air interface of the empty DAC was used. The reflectance spectra were calculated according to $R_{s-d}(\omega) = R_{dia} \times I_{s-dia}(\omega)/I_{dia}(\omega)$, where R_{dia} was estimated from the refractive index of diamond n_{dia} to 0.167 and assumed to be independent of pressure.^{19,20}

III. RESULTS AND DISCUSSION

The pressure-dependent transmittance and absorbance spectra of TiOCl for pressures up to 13.9 GPa are shown in Fig. 2; above 13.9 GPa, the transmitted signal is zero. For the lowest applied pressure pronounced absorption features are observed at around 5300 cm^{-1} (0.66 eV) and 12300 cm^{-1} (1.53 eV) in the $\mathbf{E}||a$ and $\mathbf{E}||b$ absorbance spectra, respectively [Figs. 2(c) and 2(d)]. The two absorption features can be attributed to excitations between the Ti 3d energy levels whose degeneracy is lifted by the crystal field.^{8,9} Since our transmittance measurements were carried out on very thin samples (thickness ≤ 5 μm), we could determine the precise positions and shapes of the two orbital excitations. Both absorption peaks are symmetric and can be described by a Gaussian line shape. (For fitting the orbital excitation around 12300 cm^{-1} , an exponential function describing the Urbach tail of the charge gap²¹ was taken into account.) The broadening resulting in a Gaussian profile is ascribed to vibrational excitations accompanying the electronic transitions.²²

With increasing pressure the orbital excitations broaden and continuously shift to higher frequencies (see Fig. 3). The frequency shifts indicate an increasing crystal field splitting

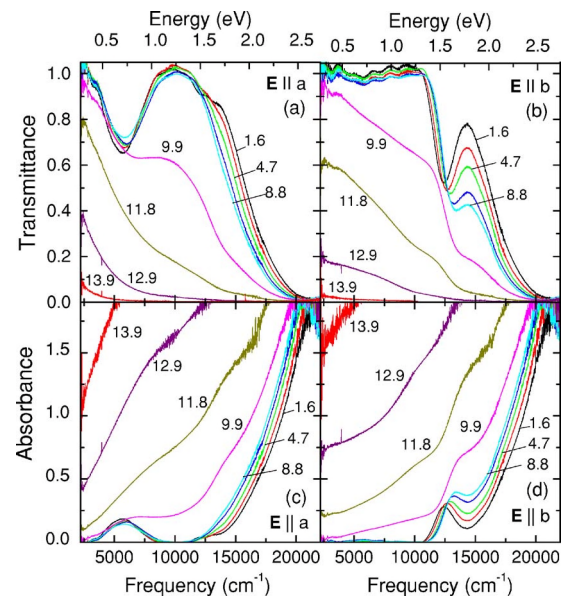


FIG. 2. (Color online) Room-temperature transmittance $T(\omega) = I_s(\omega)/I_r(\omega)$ (see text for definitions) of TiOCl as a function of pressure for the polarization (a) $\mathbf{E}||a$ and (b) $\mathbf{E}||b$. The lower graphs show the corresponding absorbance $A = \log_{10}(1/T)$ as a function of pressure for (c) $\mathbf{E}||a$ and (d) $\mathbf{E}||b$. The numbers indicate the applied pressures in GPa.

of the Ti 3d levels, which is most probably due to pressure-induced changes of the crystal structure, like modifications of the strong distortions of the $[\text{TiO}_4\text{Cl}_2]$ octahedra. However, due to the lack of crystal structure data under pressure, we can only speculate on this issue.

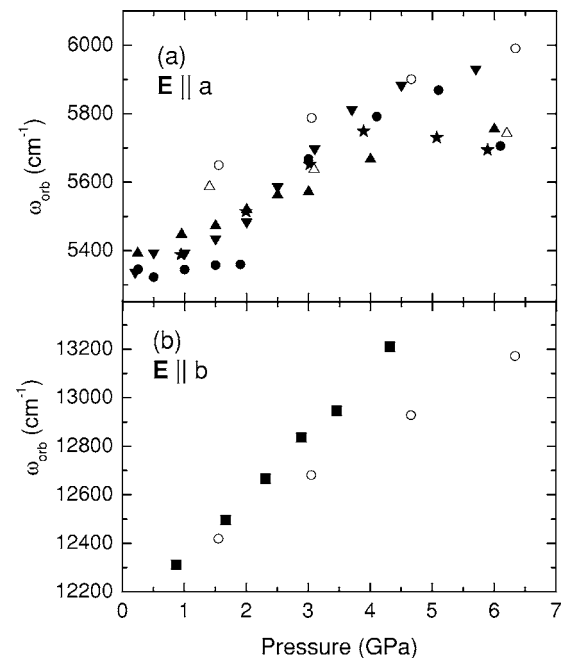


FIG. 3. Pressure-dependent positions of the orbital excitations of TiOCl, shifting to higher frequencies with increasing pressure, for (a) $\mathbf{E}||a$ and (b) $\mathbf{E}||b$. Different symbols correspond to different measurements.

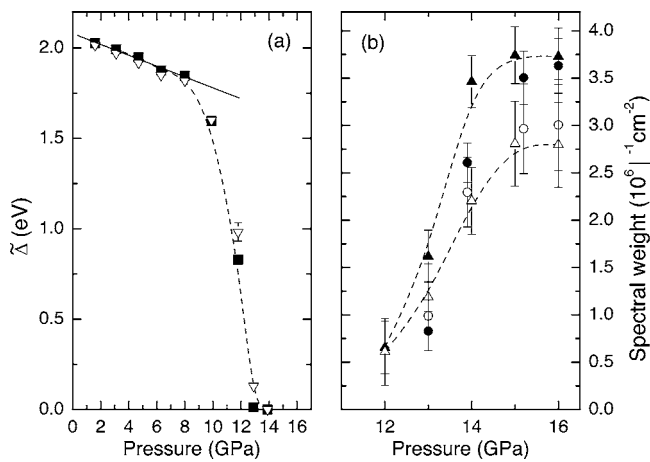


FIG. 4. (a) Charge gap $\tilde{\Delta}$ (see text for definition) as a function of pressure for $\mathbf{E}||a$ (solid symbols) and $\mathbf{E}||b$ (open symbols). The solid line indicates a linear fit to the data; the dashed line is a guide to the eye. (b) Pressure dependence of the spectral weight of the optical conductivity above the insulator-to-metal transition. Solid and open symbols correspond to $\mathbf{E}||a$ and $\mathbf{E}||b$, respectively. The same symbols indicate results from the same experimental run. Dashed lines are guides to the eye.

The rise of the absorbance above $16\,000 \text{ cm}^{-1}$ ($\approx 2 \text{ eV}$) at the lowest pressure [see Figs. 2(c) and 2(d)] can be attributed to excitations across the charge gap.^{8,9} We roughly estimated the charge gap $\tilde{\Delta}$ by a linear extrapolation (not shown) of the absorption edge. Starting from the lowest applied pressure, $\tilde{\Delta}$ initially exhibits a small linear decrease of about $240 \text{ cm}^{-1}/\text{GPa}$ [see Fig. 4(a)]. However, above 8 GPa the absorption edge rapidly shifts to lower frequencies (see also Fig. 2), indicating the abrupt closure of the charge gap. Above $\approx 12 \text{ GPa}$ the $\mathbf{E}||a,b$ transmittance is suppressed over the whole studied frequency range and the overall absorbance is strongly enhanced at these high pressures (Fig. 2).

Associated with the rapid reduction of the charge gap is a change of the sample color. Figure 5 depicts the view on the

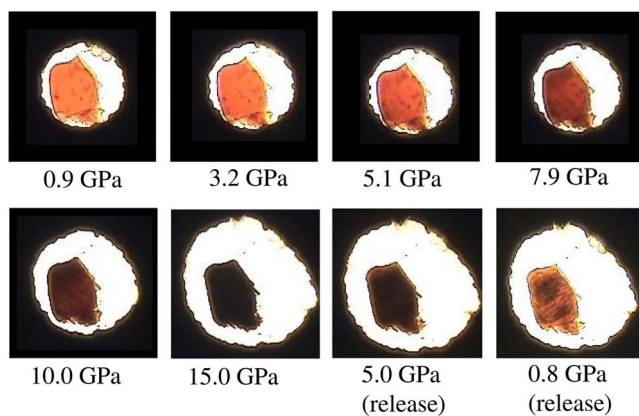


FIG. 5. (Color online) View inside the diamond anvil cell during the pressure-dependent optical measurements. With increasing pressure the sample color changes from red (gray) to black. Upon pressure release the sample does not completely recover its original color.

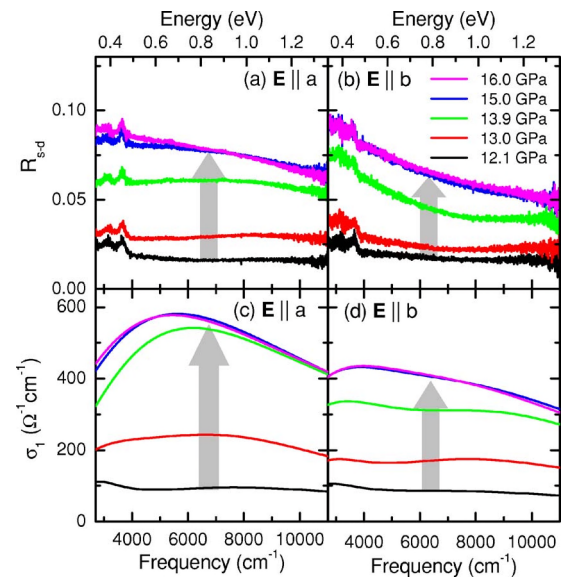


FIG. 6. (Color online) Room-temperature reflectance spectra $R_{s-d}(\omega)$ as a function of pressure for the polarization (a) $\mathbf{E}||a$ and (b) $\mathbf{E}||b$. The lower graphs show the corresponding real part $\sigma_1(\omega)$ of the optical conductivity obtained by fitting of the $R_{s-d}(\omega)$ data with the Drude-Lorentz model for (c) $\mathbf{E}||a$ and (d) $\mathbf{E}||b$. Arrows indicate the changes with increasing pressure.

sample inside the DAC at different pressures: At ambient pressure the sample appears red, since only incident radiation with frequencies below the charge gap ($\approx 2 \text{ eV}$) is transmitted. Due to the strong suppression of the transmittance above $\approx 9 \text{ GPa}$, the sample color changes from red to black. Upon pressure release the sample does not completely recover its original color, as illustrated by some parts of the sample remaining black. It thus seems that the pressure-induced reduction of the charge gap is not reversible, at least in parts of the sample (irrespective of the pressure-transmitting medium used).

Since TiOCl becomes opaque for pressures above $\approx 12 \text{ GPa}$, we completed our spectroscopic study with pressure-dependent reflectance measurements in the near-infrared range for $\mathbf{E}||a,b$ [see Figs. 6(a) and 6(b)].²³ For pressures below 12 GPa the reflectance $R_{s-d}(\omega)$ is very low (about 3%); it cannot be correctly analyzed due to partial transparency of the sample, as demonstrated by the interference fringes in the reflectance spectra due to multiple reflections within the sample (not shown). With increasing pressure the interference fringes disappear and, most importantly, at around 12 GPa, $R_{s-d}(\omega)$ abruptly increases in the whole studied frequency range for both polarization directions. We ascribe this abrupt increase to additional excitations in the infrared range induced for pressures above 12 GPa. In order to determine their contribution to the optical conductivity of the sample, we fitted the reflectance spectra with the Drude-Lorentz model,²⁴ as demonstrated in Ref. 25. The additional excitations were described by a Drude term and two Lorentz oscillators, associated with a midinfrared peak. The real part $\sigma_1(\omega)$ of the optical conductivity obtained from the fitting is shown in Figs. 6(c) and 6(d). One clearly observes the rapid onset of a broad midinfrared absorption band above 12 GPa for both polarizations.

To obtain a measure of the spectral weight of the pressure-induced excitations, we integrated the real part $\sigma_1(\omega)$ of the optical conductivity between 3000 and 10 000 cm^{-1} . Figure 4(b) shows the so-obtained spectral weight as a function of pressure above 12 GPa for both polarizations. It increases approximately linearly with increasing pressure and appears to saturate above ≈ 15 GPa. Together with the concomitant abrupt closure of the charge gap at around 12 GPa [see Fig. 4(a)], this demonstrates the transitionlike character of the pressure-induced changes in the optical response. The exact determination of the spectral weight transfer from the charge gap excitations to the Drude term and midinfrared peak requires pressure-dependent reflectance data over a broader frequency range; this will be the subject of a future study.

Our results—the suppression of transmittance accompanied by a change of the sample color and the increase of reflectance—suggest that a metallic state is induced in the Mott-Hubbard insulator TiOCl at high pressure. This pressure-induced insulator-to-metal transition can be interpreted in terms of two possible scenarios which we discuss in the following. (i) The appearance of additional absorption features inside the Mott-Hubbard gap reminds one of the optical response for a Mott transition^{26,27}: While entering the metallic state, spectral weight is transferred from the frequency range above the charge gap inside the gap, and thus a coherent Drude-like term and an incoherent midinfrared band evolves. The application of pressure (either external or chemical—i.e., by modifying the chemical composition) in general influences the bond lengths and bond angles, and hence modifies the width of the electronic bands near the Fermi energy. Such a bandwidth-controlled insulator-to-metal transition induced by *chemical* pressure is observed in various inorganic and organic compounds, and its spectroscopic signatures were demonstrated just recently.^{28,29} Our finding of inner-gap excitations in the high-pressure range with increasing spectral weight would be compatible with such a scenario.

On the other hand, for a bandwidth-controlled insulator-to-metal transition the induced changes are expected to occur more gradual than observed for TiOCl (see, for example, the abrupt decrease of the charge gap above ≈ 8 GPa

[Fig. 4(a)]). Together with the obvious nonreversible character of the transition (see Fig. 5) this hints at the second scenario (ii): the occurrence of a structural phase transition accompanied by a metallic character. Unfortunately, crystal structure data of TiOCl under pressure are currently not available, and therefore a final conclusion is not possible. Clearly, a detailed study of the pressure-induced changes of the crystal structure is needed, in order to clarify the mechanism responsible for the insulator-to-metal transition in TiOCl under pressure.

CONCLUSION

In conclusion, we studied the pressure dependence of the optical response of low-dimensional insulating TiOCl in the infrared and visible frequency range at room temperature. The orbital excitations located at ambient pressure at around 0.66 and 1.53 eV for the polarizations $\mathbf{E}||a$ and $\mathbf{E}||b$, respectively, broaden and shift to higher frequencies with increasing pressure. The pressure-induced frequency shifts indicate an increasing crystal field splitting of the Ti 3*d* energy levels suggestive for crystal structure changes. Both orbital absorption features are symmetric and have a Gaussian line shape. With increasing pressure, a strong suppression of the transmittance in the infrared and visible energy range and a change of the sample color are observed. We attribute these effects to a rapid reduction of the charge gap. At ≈ 12 GPa the near-infrared reflectance spectra for both studied polarizations abruptly increase. This is attributed to additional excitations in the infrared frequency range, which can be described by a Drude term and a midinfrared absorption band. All these observations suggest an insulator-to-metal transition in TiOCl induced at high pressure. This finding makes TiOCl an interesting candidate to search for unconventional superconductivity as earlier proposed.

ACKNOWLEDGMENTS

We thank M. Dressel for stimulating discussions. Financial support by the DFG through the Emmy Noether-program and SFB 484 is acknowledged.

*Electronic address: christine.kuntscher@physik.uni-augsburg.de

†Present address: Lehrstuhl für Experimentalphysik II, Universität Augsburg, Universitätsstr. 1, 86159 Augsburg, Germany.

¹R. J. Beynon and J. A. Wilson, *J. Phys.: Condens. Matter* **5**, 1983 (1993).

²A. Seidel, C. A. Marianetti, F. C. Chou, B. Ceder, and P. A. Lee, *Phys. Rev. B* **67**, 020405(R) (2003).

³V. Kataev, J. Baier, A. Möller, L. Jongen, G. Meyer, and A. Freimuth, *Phys. Rev. B* **68**, 140405(R) (2003).

⁴M. Shaz, S. van Smaalen, L. Palatinus, M. Hoinkis, M. Klemm, S. Horn, and R. Claessen, *Phys. Rev. B* **71**, 100405(R) (2005).

⁵T. Imai and F. C. Chou, cond-mat/0301425 (unpublished).

⁶T. Saha-Dasgupta, R. Valentí, H. Rosner, and C. Gros, *Europhys. Lett.* **67**, 63 (2004).

⁷P. Lemmens, K. Y. Choi, G. Caimi, L. Degiorgi, N. N. Kovaleva, A. Seidel, and F. C. Chou, *Phys. Rev. B* **70**, 134429 (2004).

⁸R. Rückamp, J. Baier, M. Kriener, M. W. Haverkort, T. Lorenz, G. S. Uhrig, L. Jongen, A. Möller, G. Meyer, and M. Grüninger, *Phys. Rev. Lett.* **95**, 097203 (2005).

⁹R. Rückamp, E. Benckiser, M. W. Haverkort, H. Roth, T. Lorenz, A. Freimuth, L. Jongen, A. Möller, G. Meyer, P. Reutler, B. Büchner, A. Revcolevschi, S.-W. Cheong, C. Sekar, G. Krabbes, and M. Grüninger, *New J. Phys.* **7**, 144 (2005).

¹⁰M. Hoinkis, M. Sing, J. Schäfer, M. Klemm, S. Horn, H. Benthien, E. Jeckelmann, T. Saha-Dasgupta, L. Pisani, R. Valentí, and R. Claessen, *Phys. Rev. B* **72**, 125127 (2005).

- ¹¹D. V. Zakharov, J. Deisenhofer, H.-A. Krug von Nidda, P. Lunkenheimer, J. Hemberger, M. Hoinkis, M. Klemm, M. Sing, R. Claessen, M. V. Eremin, S. Horn, and A. Loidl, *Phys. Rev. B* **73**, 094452 (2006).
- ¹²A. Krimmel, J. Strempler, B. Bohnenbuck, B. Keimer, M. Hoinkis, M. Klemm, S. Horn, A. Loidl, M. Sing, R. Claessen, and M. v. Zimmermann, *Phys. Rev. B* **73**, 172413 (2006).
- ¹³S. van Smaalen, L. Palatinus, and A. Schönleber, *Phys. Rev. B* **72**, 020105(R) (2005).
- ¹⁴L. Craco, M. S. Laad, and E. Müller-Hartmann, cond-mat/0410472 (unpublished).
- ¹⁵H. Schäfer, F. Wartenpfehl, and E. Weise, *Z. Anorg. Allg. Chem.* **295**, 268 (1958).
- ¹⁶C. A. Kuntscher, S. Frank, A. Pashkin, M. Hoinkis, M. Klemm, M. Sing, S. Horn, and R. Claessen (unpublished).
- ¹⁷I. Loa, U. Schwarz, M. Hanfland, R. K. Kremer, and K. Syassen, *Phys. Status Solidi B* **215**, 709 (1999).
- ¹⁸H. K. Mao, J. Xu, and P. M. Bell, *J. Geophys. Res.*, [Atmos.] **91**, 4673 (1986).
- ¹⁹M. I. Erements and Y. A. Timofeev, *Rev. Sci. Instrum.* **63**, 3123 (1992).
- ²⁰A. L. Ruoff and K. Ghandehari, in *High Pressure Science and Technology*, edited by S. C. Schmidt, J. W. Shaner, G. A. Samara, and M. Ross, AIP Conf. Proc. No. 309 (AIP, Woodbury, NY, 1994), pp. 1523–1525.
- ²¹F. Urbach, *Phys. Rev.* **92**, 1324 (1953).
- ²²B. N. Figgis and M. A. Hitchman, *Ligand Field Theory and Its Applications* (Wiley-VCH, New York, 1996).
- ²³The features around 3200 and 3600 cm^{-1} are artifacts due to multiphonon absorption by diamond and no intrinsic properties of the studied sample.
- ²⁴The background dielectric constant $\epsilon_{\infty}=3.7$ was determined by a Drude-Lorentz fit of ambient-pressure reflectivity data measured on a free-standing thick sample and assumed to be pressure independent.
- ²⁵C. A. Kuntscher, S. Frank, I. Loa, K. Syassen, T. Yamauchi, and Y. Ueda, *Phys. Rev. B* **71**, 220502(R) (2005).
- ²⁶M. Imada, A. Fujimori, and Y. Tokura, *Rev. Mod. Phys.* **70**, 1039 (1998).
- ²⁷M. J. Rozenberg, G. Kotliar, and H. Kajueter, *Phys. Rev. B* **54**, 8452 (1996).
- ²⁸I. Kézsmárki, N. Hanasaki, D. Hashimoto, S. Iguchi, Y. Taguchi, S. Miyasaka, and Y. Tokura, *Phys. Rev. Lett.* **93**, 266401 (2004).
- ²⁹I. Kézsmárki, N. Hanasaki, K. Watanabe, S. Iguchi, Y. Taguchi, S. Miyasaka, and Y. Tokura, *Phys. Rev. B* **73**, 125122 (2006).